



Observation of $D_{s1}(2536)^+ \rightarrow D^+ \pi^- K^+$

K. Abe,⁹ K. Abe,⁴⁷ I. Adachi,⁹ H. Aihara,⁴⁹ K. Aoki,²³ K. Arinstein,² Y. Asano,⁵⁴
 T. Aso,⁵³ V. Aulchenko,² T. Aushev,¹³ T. Aziz,⁴⁵ S. Bahinipati,⁵ A. M. Bakich,⁴⁴
 V. Balagura,¹³ Y. Ban,³⁶ S. Banerjee,⁴⁵ E. Barberio,²² M. Barbero,⁸ A. Bay,¹⁹ I. Bedny,²
 U. Bitenc,¹⁴ I. Bizjak,¹⁴ S. Blyth,²⁵ A. Bondar,² A. Bozek,²⁹ M. Bračko,^{9, 21, 14}
 J. Brodzicka,²⁹ T. E. Browder,⁸ M.-C. Chang,⁴⁸ P. Chang,²⁸ Y. Chao,²⁸ A. Chen,²⁵
 K.-F. Chen,²⁸ W. T. Chen,²⁵ B. G. Cheon,⁴ C.-C. Chiang,²⁸ R. Chistov,¹³ S.-K. Choi,⁷
 Y. Choi,⁴³ Y. K. Choi,⁴³ A. Chuvikov,³⁷ S. Cole,⁴⁴ J. Dalseno,²² M. Danilov,¹³ M. Dash,⁵⁶
 L. Y. Dong,¹¹ R. Dowd,²² J. Dragic,⁹ A. Drutskoy,⁵ S. Eidelman,² Y. Enari,²³ D. Epifanov,²
 F. Fang,⁸ S. Fratina,¹⁴ H. Fujii,⁹ N. Gabyshev,² A. Garmash,³⁷ T. Gershon,⁹ A. Go,²⁵
 G. Gokhroo,⁴⁵ P. Goldenzweig,⁵ B. Golob,^{20, 14} A. Gorišek,¹⁴ M. Grosse Perdekamp,³⁸
 H. Guler,⁸ R. Guo,²⁶ J. Haba,⁹ K. Hara,⁹ T. Hara,³⁴ Y. Hasegawa,⁴² N. C. Hastings,⁴⁹
 K. Hasuko,³⁸ K. Hayasaka,²³ H. Hayashii,²⁴ M. Hazumi,⁹ T. Higuchi,⁹ L. Hinz,¹⁹ T. Hojo,³⁴
 T. Hokuue,²³ Y. Hoshi,⁴⁷ K. Hoshina,⁵² S. Hou,²⁵ W.-S. Hou,²⁸ Y. B. Hsiung,²⁸
 Y. Igarashi,⁹ T. Iijima,²³ K. Ikado,²³ A. Imoto,²⁴ K. Inami,²³ A. Ishikawa,⁹ H. Ishino,⁵⁰
 K. Itoh,⁴⁹ R. Itoh,⁹ M. Iwasaki,⁴⁹ Y. Iwasaki,⁹ C. Jacoby,¹⁹ C.-M. Jen,²⁸ R. Kagan,¹³
 H. Kakuno,⁴⁹ J. H. Kang,⁵⁷ J. S. Kang,¹⁶ P. Kapusta,²⁹ S. U. Kataoka,²⁴ N. Katayama,⁹
 H. Kawai,³ N. Kawamura,¹ T. Kawasaki,³¹ S. Kazi,⁵ N. Kent,⁸ H. R. Khan,⁵⁰
 A. Kibayashi,⁵⁰ H. Kichimi,⁹ H. J. Kim,¹⁸ H. O. Kim,⁴³ J. H. Kim,⁴³ S. K. Kim,⁴¹
 S. M. Kim,⁴³ T. H. Kim,⁵⁷ K. Kinoshita,⁵ N. Kishimoto,²³ S. Korpar,^{21, 14} Y. Kozakai,²³
 P. Krizan,^{20, 14} P. Krokovny,⁹ T. Kubota,²³ R. Kulasiri,⁵ C. C. Kuo,²⁵ H. Kurashiro,⁵⁰
 E. Kurihara,³ A. Kusaka,⁴⁹ A. Kuzmin,² Y.-J. Kwon,⁵⁷ J. S. Lange,⁶ G. Leder,¹²
 S. E. Lee,⁴¹ Y.-J. Lee,²⁸ T. Lesiak,²⁹ J. Li,⁴⁰ A. Limosani,⁹ S.-W. Lin,²⁸ D. Liventsev,¹³
 J. MacNaughton,¹² G. Majumder,⁴⁵ F. Mandl,¹² D. Marlow,³⁷ H. Matsumoto,³¹
 T. Matsumoto,⁵¹ A. Matyja,²⁹ Y. Mikami,⁴⁸ W. Mitaroff,¹² K. Miyabayashi,²⁴ H. Miyake,³⁴
 H. Miyata,³¹ Y. Miyazaki,²³ R. Mizuk,¹³ D. Mohapatra,⁵⁶ G. R. Moloney,²² T. Mori,⁵⁰
 A. Murakami,³⁹ T. Nagamine,⁴⁸ Y. Nagasaka,¹⁰ T. Nakagawa,⁵¹ I. Nakamura,⁹
 E. Nakano,³³ M. Nakao,⁹ H. Nakazawa,⁹ Z. Natkaniec,²⁹ K. Neichi,⁴⁷ S. Nishida,⁹
 O. Nitoh,⁵² S. Noguchi,²⁴ T. Nozaki,⁹ A. Ogawa,³⁸ S. Ogawa,⁴⁶ T. Ohshima,²³ T. Okabe,²³
 S. Okuno,¹⁵ S. L. Olsen,⁸ Y. Onuki,³¹ W. Ostrowicz,²⁹ H. Ozaki,⁹ P. Pakhlov,¹³ H. Palka,²⁹
 C. W. Park,⁴³ H. Park,¹⁸ K. S. Park,⁴³ N. Parslow,⁴⁴ L. S. Peak,⁴⁴ M. Pernicka,¹²
 R. Pestotnik,¹⁴ M. Peters,⁸ L. E. Piilonen,⁵⁶ A. Poluektov,² F. J. Ronga,⁹ N. Root,²
 M. Rozanska,²⁹ H. Sahoo,⁸ M. Saigo,⁴⁸ S. Saitoh,⁹ Y. Sakai,⁹ H. Sakamoto,¹⁷
 H. Sakaue,³³ T. R. Sarangi,⁹ M. Satapathy,⁵⁵ N. Sato,²³ N. Satoyama,⁴² T. Schietinger,¹⁹
 O. Schneider,¹⁹ P. Schönmeier,⁴⁸ J. Schümann,²⁸ C. Schwanda,¹² A. J. Schwartz,⁵
 T. Seki,⁵¹ K. Senyo,²³ R. Seuster,⁸ M. E. Sevier,²² T. Shibata,³¹ H. Shibuya,⁴⁶
 J.-G. Shiu,²⁸ B. Shwartz,² V. Sidorov,² J. B. Singh,³⁵ A. Somov,⁵ N. Soni,³⁵ R. Stamen,⁹

S. Stanič,³² M. Starič,¹⁴ A. Sugiyama,³⁹ K. Sumisawa,⁹ T. Sumiyoshi,⁵¹ S. Suzuki,³⁹
 S. Y. Suzuki,⁹ O. Tajima,⁹ N. Takada,⁴² F. Takasaki,⁹ K. Tamai,⁹ N. Tamura,³¹
 K. Tanabe,⁴⁹ M. Tanaka,⁹ G. N. Taylor,²² Y. Teramoto,³³ X. C. Tian,³⁶ K. Trabelsi,⁸
 Y. F. Tse,²² T. Tsuboyama,⁹ T. Tsukamoto,⁹ K. Uchida,⁸ Y. Uchida,⁹ S. Uehara,⁹
 T. Uglov,¹³ K. Ueno,²⁸ Y. Unno,⁹ S. Uno,⁹ P. Urquijo,²² Y. Ushiroda,⁹ G. Varner,⁸
 K. E. Varvell,⁴⁴ S. Villa,¹⁹ C. C. Wang,²⁸ C. H. Wang,²⁷ M.-Z. Wang,²⁸ M. Watanabe,³¹
 Y. Watanabe,⁵⁰ L. Widhalm,¹² C.-H. Wu,²⁸ Q. L. Xie,¹¹ B. D. Yabsley,⁵⁶ A. Yamaguchi,⁴⁸
 H. Yamamoto,⁴⁸ S. Yamamoto,⁵¹ Y. Yamashita,³⁰ M. Yamauchi,⁹ Heyoung Yang,⁴¹
 J. Ying,³⁶ S. Yoshino,²³ Y. Yuan,¹¹ Y. Yusa,⁴⁸ H. Yuta,¹ S. L. Zang,¹¹ C. C. Zhang,¹¹
 J. Zhang,⁹ L. M. Zhang,⁴⁰ Z. P. Zhang,⁴⁰ V. Zhilich,² T. Ziegler,³⁷ and D. Zürcher¹⁹

(The Belle Collaboration)

¹*Aomori University, Aomori*

²*Budker Institute of Nuclear Physics, Novosibirsk*

³*Chiba University, Chiba*

⁴*Chonnam National University, Kwangju*

⁵*University of Cincinnati, Cincinnati, Ohio 45221*

⁶*University of Frankfurt, Frankfurt*

⁷*Gyeongang National University, Chinju*

⁸*University of Hawaii, Honolulu, Hawaii 96822*

⁹*High Energy Accelerator Research Organization (KEK), Tsukuba*

¹⁰*Hiroshima Institute of Technology, Hiroshima*

¹¹*Institute of High Energy Physics,*

Chinese Academy of Sciences, Beijing

¹²*Institute of High Energy Physics, Vienna*

¹³*Institute for Theoretical and Experimental Physics, Moscow*

¹⁴*J. Stefan Institute, Ljubljana*

¹⁵*Kanagawa University, Yokohama*

¹⁶*Korea University, Seoul*

¹⁷*Kyoto University, Kyoto*

¹⁸*Kyungpook National University, Taegu*

¹⁹*Swiss Federal Institute of Technology of Lausanne, EPFL, Lausanne*

²⁰*University of Ljubljana, Ljubljana*

²¹*University of Maribor, Maribor*

²²*University of Melbourne, Victoria*

²³*Nagoya University, Nagoya*

²⁴*Nara Women's University, Nara*

²⁵*National Central University, Chung-li*

²⁶*National Kaohsiung Normal University, Kaohsiung*

²⁷*National United University, Miao Li*

²⁸*Department of Physics, National Taiwan University, Taipei*

²⁹*H. Niewodniczanski Institute of Nuclear Physics, Krakow*

³⁰*Nippon Dental University, Niigata*

³¹*Niigata University, Niigata*

³²*Nova Gorica Polytechnic, Nova Gorica*

³³*Osaka City University, Osaka*

³⁴*Osaka University, Osaka*

- ³⁵*Panjab University, Chandigarh*
³⁶*Peking University, Beijing*
³⁷*Princeton University, Princeton, New Jersey 08544*
³⁸*RIKEN BNL Research Center, Upton, New York 11973*
³⁹*Saga University, Saga*
⁴⁰*University of Science and Technology of China, Hefei*
⁴¹*Seoul National University, Seoul*
⁴²*Shinshu University, Nagano*
⁴³*Sungkyunkwan University, Suwon*
⁴⁴*University of Sydney, Sydney NSW*
⁴⁵*Tata Institute of Fundamental Research, Bombay*
⁴⁶*Toho University, Funabashi*
⁴⁷*Tohoku Gakuin University, Tagajo*
⁴⁸*Tohoku University, Sendai*
⁴⁹*Department of Physics, University of Tokyo, Tokyo*
⁵⁰*Tokyo Institute of Technology, Tokyo*
⁵¹*Tokyo Metropolitan University, Tokyo*
⁵²*Tokyo University of Agriculture and Technology, Tokyo*
⁵³*Toyama National College of Maritime Technology, Toyama*
⁵⁴*University of Tsukuba, Tsukuba*
⁵⁵*Utkal University, Bhubaneswer*
⁵⁶*Virginia Polytechnic Institute and State University, Blacksburg, Virginia 24061*
⁵⁷*Yonsei University, Seoul*

Abstract

We report the observation of the decay $D_{s1}(2536)^+ \rightarrow D^+\pi^-K^+$. We also measure the helicity angle distributions in the decay $D_{s1}(2536) \rightarrow D^{*+}K_S^0$ and thus constrain the contributions and the phase difference of D and S wave amplitudes in this decay. The results are based on a 281 fb^{-1} data sample collected with the Belle detector near the $\Upsilon(4S)$ resonance, at the KEKB asymmetric energy e^+e^- collider.

PACS numbers:

INTRODUCTION

Two states $D_{sJ}(2317)^+$ and $D_{sJ}(2460)^+$ have been discovered recently both in continuum e^+e^- annihilation near $\sqrt{s} = 10.6$ GeV/ c^2 and in B meson decays [1], [2]. Their decay properties are consistent with the assumption that these are $J^P = 0^+, 1^+$ states with $j = L + S_{\bar{s}} = 1/2$. Here $L = 1$ is the orbital momentum, $S_{\bar{s}}$ is the spin of the light antiquark. However, their masses are unexpectedly low [3]. This has renewed interest in measurements of P-wave excited charm mesons.

We report the first observation of the decay $D_{s1}(2536)^+ \rightarrow D^+\pi^-K^+$ (the inclusion of charge conjugate modes is implied throughout the paper). The $D^+\pi^-$ pair in the final state is the only $D\pi$ combination that cannot come from a D^* resonance. Note that D^{*0} mesons can only be produced virtually here since $M_{D^{*0}} < M_{D^+} + M_{\pi^-}$. The $D_{s1}(2536)^+ \rightarrow D^+\pi^-K^+$ and $D_{s1}(2536)^+ \rightarrow D_s^+\pi^+\pi^-$ [2] modes are the only known three-body decays of the $D_{s1}(2536)^+$.

In addition, we have performed an angular analysis of the $D_{s1}(2536)^+ \rightarrow D^{*+}K_S^0$ mode. In the limit of infinite c quark mass this decay of a $J^P = 1^+, j = 3/2$ state should proceed via a pure D-wave [4]. The corresponding decay of its partner, the $D_{sJ}(2460)^+$, which is believed to be a $1^+, j = 1/2$ state is energetically forbidden, but if it were allowed it would proceed via a pure S wave. Since heavy quark symmetry is not exact, the two 1^+ states can mix with each other. In particular, an S wave component can appear in the decay $D_{s1}(2536)^+ \rightarrow D^*K$. Moreover, even if the mixing is small, the S wave component can give a sizeable contribution to the width because the D wave contribution is strongly suppressed by the small energy release in the $D_{s1}(2536)^+ \rightarrow D^*K$ decay. The angular decomposition in S and D waves for the analogous decays of the $1^+, j = 3/2$ $D_1(2420)^{0,+}$ mesons to $D^{*+}\pi^-$, $D^{*0}\pi^+$ was performed more than 10 years ago by CLEO [5], but currently no results on the $D_{s1}(2536)^+$ exist.

This study is based on a data sample of 253fb^{-1} collected at the $\Upsilon(4S)$ resonance and 28fb^{-1} at an energy 60 MeV below the resonance with the Belle detector at the KEKB asymmetric-energy e^+e^- (3.5 on 8 GeV) collider [6]. The Belle detector is a large-solid-angle magnetic spectrometer that consists of a silicon vertex detector (SVD), a 50-layer central drift chamber (CDC), an array of aerogel threshold Čerenkov counters (ACC), a barrel-like arrangement of time-of-flight scintillation counters (TOF), and an electromagnetic calorimeter comprised of CsI(Tl) crystals (ECL) located inside a super-conducting solenoid coil that provides a 1.5 T magnetic field. An iron flux-return located outside of the coil is instrumented to detect K_L^0 mesons and to identify muons (KLM). The detector is described in detail elsewhere [7]. Two inner detector configurations were used. A 2.0 cm beampipe and a 3-layer silicon vertex detector was used for the first sample of 155fb^{-1} , while a 1.5 cm beampipe, a 4-layer silicon detector and a small-cell inner drift chamber were used to record the remaining 126fb^{-1} [8].

In Monte Carlo, $D_{s1}(2536)^+$ from e^+e^- annihilation, particle decays and the detailed detector response is simulated using the **PYTHIA**, **EvtGen** and **GEANT** packages [9] respectively. The D^0 and D^+ decay modes used in reconstruction are generated with their resonant substructures taken from the PDG [10] but neglecting any interference effects. The width of the $D_{s1}(2536)^+$ resonance in the simulation is set to zero. Only the D wave matrix element is used for the $D_{s1}(2536)^+ \rightarrow D^{*+}K_S^0$ decay. As is shown below no clear resonant substructure is visible in the decay $D_{s1}(2536)^+ \rightarrow D^+\pi^-K^+$. Therefore, it is simulated as a three-body phase space decay.

$$D_{s1}(2536)^+ \rightarrow D^+\pi^-K^+ \text{ DECAY AND CALCULATION OF } \frac{\mathcal{B}(D_{s1}^+ \rightarrow D^+\pi^-K^+)}{\mathcal{B}(D_{s1}^+ \rightarrow D^{*+}K^0)}.$$

π^\pm and K^\pm candidates are required to originate from the vicinity of the event dependent interaction point. To identify kaons, the dE/dx , time of flight and Čerenkov light yield information for each track are combined to form kaon \mathcal{L}_K and pion \mathcal{L}_π likelihoods and the requirement $\mathcal{L}_K/(\mathcal{L}_K + \mathcal{L}_\pi) > 0.1$ is imposed. K_S^0 candidates are reconstructed via the $\pi^+\pi^-$ decay channel. D^0 and D^+ mesons are reconstructed using $K^-\pi^+$, $K_S^0\pi^+\pi^-$, $K^-\pi^+\pi^+\pi^-$ and $K_S^0\pi^+$, $K^-\pi^+\pi^+$ decay modes, respectively. All combinations with masses within ± 20 MeV/c² of the nominal D mass are selected and then a mass and vertex constrained fit is applied.

Candidate D^{*+} 's are reconstructed using the $D^0\pi^+$ mode. The slow π^+ momentum resolution suffers from multiple scattering. It is improved by a track refit procedure in which the π^+ origin point is constrained by the intersection of the D momentum and the known region of e^+e^- interactions. The same procedure is applied to the slow π^- and K^+ from the $D_{s1}(2536)^+ \rightarrow D^+\pi^-K^+$ decay. The $M_{D^0\pi^+}$ mass is required to be within ± 1.5 MeV/c² around the D^{*+} nominal value. The D^{*+} mass constraint fit is not applied. Instead, the mass difference $M_{D^0\pi^+K_S^0} - M_{D^0\pi^+}$ is used for $D_{s1}(2536)^+$ where the errors in D^{*+} momentum essentially cancel out.

It is known that the momentum spectrum of the excited charm resonances from continuum e^+e^- annihilation is hard. In addition, due to the strong magnetic field in BELLE the reconstruction efficiency for slow π^\pm and K^+ mesons is larger for higher $D_{s1}(2536)^+$ momenta. Therefore, to reduce the combinatorial background, it is required that $x_P > 0.8$, where the scaled momentum x_P is defined as $x_P = p^*/p_{\max}^*$. Here p^* is the momentum of the $D_{s1}(2536)^+$ candidate in the e^+e^- center of mass frame. p_{\max}^* is the momentum which the candidate would have if it carried all of the beam energy E_{beam}^* in the same frame: $p_{\max}^* = \sqrt{E_{\text{beam}}^{*2} - M^2}$.

The mass $M_{D^+\pi^-K^+}$ and the mass difference $(M_{D^0\pi^+K_S^0} - M_{D^0\pi^+}) + M_{D^{*+}}^{\text{PDG}}$ for all accepted combinations are plotted in Fig. 1. Here and in the following the PDG superscript denotes the nominal mass value from [10]. A clear peak for the new decay channel $D_{s1}(2536)^+ \rightarrow D^+\pi^-K^+$ is visible in Fig. 1. The mass spectrum of the wrong sign combinations $D^+\pi^+K^-$ shown by the hatched histogram has no enhancement in the $D_{s1}(2536)^+$ region.

To calculate the number of $D_{s1}(2536)^+$ decays, the distributions in Fig. 1 are fit to the sum of two Gaussians. Their central values are required to be equal. To ensure that the second Gaussian is always wider than the first one, its width is chosen to be of the form $\sigma_2 = \sqrt{\sigma_1^2 + \Delta\sigma^2}$. The position of the peak, σ_1 , $\Delta\sigma$, the fraction of events in the first Gaussian and the total number of events in two Gaussians are allowed to vary in the fit. The background for the three-body $D^+\pi^-K^+$ mode is parameterized by the second order polynomial multiplied by the function $(M - M_{D^+\pi^-K^+}^{\text{threshold}})^2$, where $M_{D^+\pi^-K^+}^{\text{threshold}} = M_{D^+}^{\text{PDG}} + M_{\pi^-}^{\text{PDG}} + M_{K^+}^{\text{PDG}}$. For the two-body $D^{*+}K_S^0$ mode the background parametrization is chosen to be of the form $\sqrt{M - M_{D^{*+}K_S^0}^{\text{threshold}}}$ times a first order polynomial, where $M_{D^{*+}K_S^0}^{\text{threshold}} = M_{D^{*+}}^{\text{PDG}} + M_{K_S^0}^{\text{PDG}}$. Table I contains the fit results together with the parameters of the Gaussians obtained from Monte Carlo. There is a small fraction of events that contribute two entries to the $D_{s1}(2536)^+$ signal region in the mass plot. The last row in the Table I shows the excess of such events in comparison with the same number averaged over the left and the right sideband. The signal and the sidebands are defined as $|\Delta M_{D_{s1}^+}| < 5$ MeV/c², 10

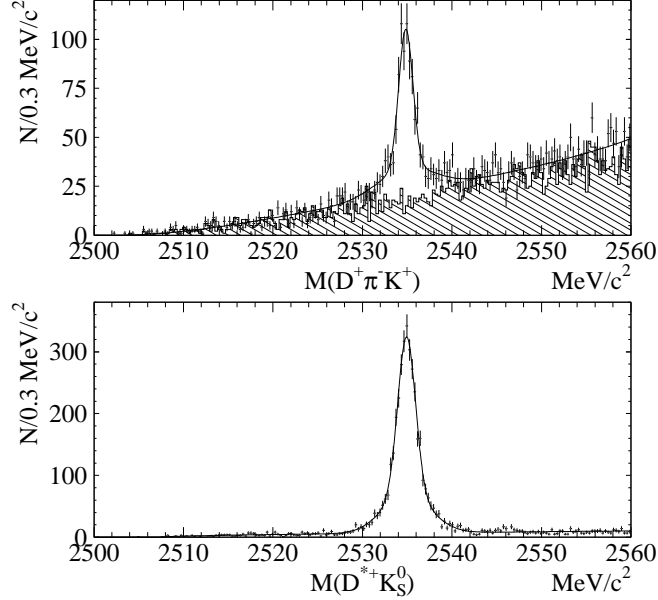


FIG. 1: $D_{s1}(2536)^+$ mass spectra for $D^+\pi^-K^+$ (top) and $D^{*+}K_S^0$ (bottom) decay modes. The latter is calculated using the mass difference $(M_{D^0\pi^+K_S^0} - M_{D^0\pi^+}) + M_{D^{*+}}^{\text{PDG}}$. The hatched histogram in the top plot shows the corresponding spectrum of wrong sign $D^+\pi^+K^-$ combinations. The fit is described in the text. The fit results are listed in Table I.

$\text{MeV}/c^2 < |\Delta M_{D_{s1}^+}| < 20 \text{ MeV}/c^2$, respectively, where $\Delta M_{D_{s1}^+}$ is measured relative to the peak position obtained from the fit to Fig. 1.

TABLE I: Fit results of the spectra shown in Fig. 1: number of events in two Gaussians, fraction of events in the narrower 1st Gaussian, σ_1 , $\Delta\sigma$ and $M_{D_{s1}} - M_{D_{s1}}^{\text{PDG}}$. The last three values are given in MeV/c^2 . Note that the value of $M_{D_{s1}}^{\text{PDG}}$ is known with errors of $\pm 0.34 \pm 0.5 \text{ MeV}/c^2$. The sigma of the 2nd Gaussian is $\sigma_2 = \sqrt{\sigma_1^2 + \Delta\sigma^2}$. The 3rd and 5th columns contain the corresponding Gaussian parameters obtained in Monte Carlo. The number of double counted events after sideband subtraction is given in the last row.

| | $(D^+\pi^-K^+)_{\text{Data}}$ | $(D^+\pi^-K^+)_{\text{MC}}$ | $(D^{*+}K_S^0)_{\text{Data}}$ | $(D^{*+}K_S^0)_{\text{MC}}$ |
|--|------------------------------------|-----------------------------|------------------------------------|-----------------------------|
| N events | 802 ± 56 | | 3474 ± 64 | |
| 1st G. fraction | 0.58 ± 0.07 | 0.769 ± 0.014 | 0.60 ± 0.04 | 0.862 ± 0.013 |
| σ_1 | 0.79 ± 0.07 | 0.478 ± 0.011 | 0.98 ± 0.04 | 0.746 ± 0.014 |
| $\Delta\sigma$ | 3.1 ± 0.6 | 1.85 ± 0.11 | 2.46 ± 0.15 | 2.49 ± 0.18 |
| $M_{D_{s1}} - M_{D_{s1}}^{\text{PDG}}$ | -0.51 ± 0.06 | 0.014 ± 0.008 | -0.42 ± 0.03 | 0.023 ± 0.012 |
| double counting | $28 - \frac{20}{2} = 18$ | | $105 - \frac{18}{2} = 96$ | |

To cross-check the results, the D^+ mass spectrum is plotted in Fig. 2 for the $D_{s1}(2536)^+$ signal and sidebands. The latter is normalized to the area of the signal interval. The sideband subtracted plot shown in the bottom of Fig. 2 is fit to a double Gaussian as above and a constant background. The resulting yield 739 ± 51 is consistent with the yield 679 ± 48

obtained from the fit of the $D_{s1}(2536)^+$ mass spectrum. The constant background level is found to be -0.4 ± 0.6 , which is consistent with zero. The enhancement in the D^+ mass region observed in the $D_{s1}(2536)^+$ sidebands (top plot of Fig. 2) is due to combinations of a real D^+ with a random $\pi^- K^+$ pair in the event.

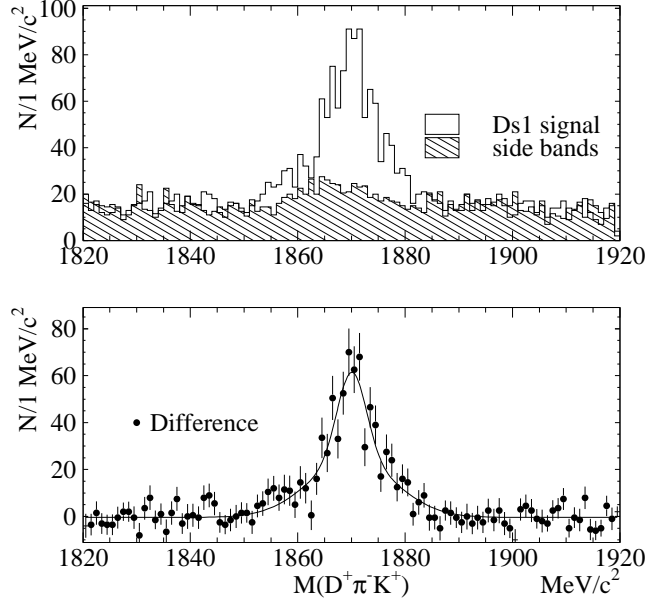


FIG. 2: D^+ mass spectrum for the $D_{s1}(2536)^+$ signal band ($|\Delta M_{D^+\pi^-K^+}| < 5 \text{ MeV}/c^2$, open histogram in the top plot) and the sidebands ($10 < |\Delta M_{D^+\pi^-K^+}| < 20 \text{ MeV}/c^2$, normalized to the signal interval, hatched histogram). Here $\Delta M_{D^+\pi^-K^+} = M_{D^+\pi^-K^+} - M_{D_{s1}}^0$, $M_{D_{s1}}^0$ is the $D_{s1}(2536)^+$ peak position in the top plot of Fig. 1. The bottom plot shows the difference. The solid curve shows the results of the fit described in the text.

Due to the low momenta of the final state particles, the $D_{s1}(2536)^+$ reconstruction efficiency strongly depends on its momentum, which is found to be harder in data than in Monte Carlo. Therefore the ratio of $D_{s1}(2536)^+$ branching fractions is calculated using the following formula:

$$\frac{\mathcal{B}(D_{s1}(2536)^+ \rightarrow D^+\pi^-K^+)}{\mathcal{B}(D_{s1}(2536)^+ \rightarrow D^{*+}K_S^0)} = \frac{(N_{D\pi K} - n_{D\pi K}^{\text{dbl cnt}})}{(N_{D^{*+}K_S^0} - n_{D^{*+}K_S^0}^{\text{dbl cnt}})} \left[\frac{\sum_{p_i} N_{D^{*+}K_S^0}^{p_i} \frac{\epsilon_{D^+\pi^-K^+}^{p_i}}{\epsilon_{D^{*+}K_S^0}^{p_i}}}{\sum_{p_i} N_{D^{*+}K_S^0}^{p_i}} \right]^{-1} \frac{\mathcal{B}(D^{*+} \rightarrow D^0\pi^+) \mathcal{B}(D^0) \mathcal{B}(K^0 \rightarrow K_S^0 \rightarrow \pi^+\pi^-)}{\mathcal{B}(D^+)}.$$

Here, $\epsilon_{D^+\pi^-K^+}^{p_i}$ and $\epsilon_{D^{*+}K_S^0}^{p_i}$ are the reconstruction efficiencies in individual momentum bins of $D_{s1}(2536)^+$, $N_{D^{*+}K_S^0}^{p_i}$ are the number of $D_{s1}(2536)^+ \rightarrow D^{*+}K_S^0$ decays observed in a given momentum bin, and the sum runs over the momentum bins with $x_P > 0.8$. $N_{D\pi K}$, $N_{D^{*+}K_S^0}$ and $n_{D\pi K}^{\text{dbl cnt}}$, $n_{D^{*+}K_S^0}^{\text{dbl cnt}}$ are the total number of decays obtained by performing the fit to the $D_{s1}(2536)^+$ mass spectra and the number of double counted events, respectively (see Table I). $\mathcal{B}(D^0, D^+)$ is the sum of branching fractions of D^0 and D^+ modes used in the

reconstruction [10]. For modes with K_S^0 's in the final state the branching fractions are in addition multiplied by $\mathcal{B}(K^0 \rightarrow K_S^0 \rightarrow \pi^+\pi^-) = \frac{1}{2} \cdot \mathcal{B}(K^0 \rightarrow \pi^+\pi^-)$. The dependence of the efficiency on the initial polarization of the $D_{s1}(2536)^+$ is checked and found to be negligible. The efficiency does not depend on the D^{*+} helicity angle in the $D^{*+}K_S^0$ decay and thus on the proportions of S and D waves. For the $D^+\pi^-K^+$ mode the efficiency is independent of the $D^+\pi^-$, $K^+\pi^-$ masses and the $D^+\pi^-$ helicity angle. The ratio of branching fractions is found to be

$$\frac{\mathcal{B}(D_{s1}(2536)^+ \rightarrow D^+\pi^-K^+)}{\mathcal{B}(D_{s1}(2536)^+ \rightarrow D^{*+}K^0)} = (2.8 \pm 0.2 \pm 0.4)\%.$$

The systematic error receives contribution from different sources listed in Table II. A possible difference between the data and Monte Carlo in evaluation of the tracking efficiency was estimated using partially reconstructed D^{*+} decays. The tracking errors due to slow K^+ , π^\pm and pions from K_S^0 are added linearly. The uncertainty in the kaon particle identification is estimated using D^{*+} decays. Uncertainty in the ratio of D^+ and D^0 efficiencies was determined by a comparison of different decay modes used in the reconstruction. The largest contribution to the systematic uncertainty arises due to the fitting model and was evaluated by comparing the fit results using different binnings of the $D^+\pi^-K^+$ and $D^{*+}K_S^0$ mass spectra. The largest discrepancy (in the $D^+\pi^-K^+$ decay mode) is taken as the systematic error. Finally, the contribution due to the assumption that the efficiency does not depend on the decay angles of the $D_{s1}(2536)^+$ and its initial polarization, $D\pi$ helicity angles and $M(D^+\pi^-)$ is evaluated by comparing the yields of events using either an average or differential efficiency in the specified variables. The total systematic error is found to be 12% (Table II).

TABLE II: Systematic uncertainties for $\frac{\mathcal{B}(D_{s1}(2536)^+ \rightarrow D^+\pi^-K^+)}{\mathcal{B}(D_{s1}(2536)^+ \rightarrow D^{*+}K^0)}$.

| Source | Uncertainty, % |
|--|----------------|
| Slow π^\pm tracking efficiency | 1.5 |
| Slow K^+ tracking efficiency | 1 |
| Slow K_S^0 tracking efficiency | 5 |
| Slow K^+ particle identification | 1.2 |
| Ratio of D^+ and D^0 efficiencies | 3.5 |
| Fit to $M(D^+\pi^-K^+)$ distribution | 8.5 |
| Efficiency independence on $D_{s1}(2536)^+$ polarization, $D\pi$ helicity angle and $M(D^+\pi^-)$ | 1.1 |
| Total | 12.0 |

The $D^+\pi^-$ and $K^+\pi^-$ mass distributions for the $D_{s1}(2536)^+ \rightarrow D^+\pi^-K^+$ decay are shown in Fig. 3. The $D_{s1}(2536)^+$ signal yield is obtained from fits to the $D^+\pi^-K^+$ mass distribution in bins of $D^+\pi^-$ and $K^+\pi^-$ mass. All Gaussian parameters except the total number of events are fixed in the fit to the values obtained from Fig. 1. The position of the threshold used for the background description depends on the chosen bin. The areas of the plots have been normalized to unity. The plots are not efficiency corrected since the differential efficiency does not depend on $D^+\pi^-$ or $K^+\pi^-$ masses to within the errors of Monte Carlo statistics. No dominant resonant substructure is visible in Fig. 3.

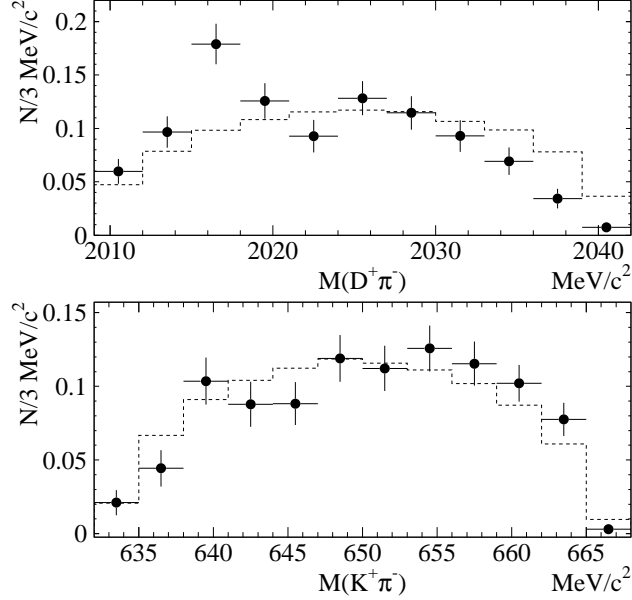


FIG. 3: Normalized mass spectra of $D^+\pi^-$ (top) and $K^+\pi^-$ (bottom) pairs from $D_{s1}(2536)^+ \rightarrow D^+\pi^-K^+$ decay obtained from fits to the $D^+\pi^-K^+$ mass distributions in different $D^+\pi^-$ or $K^+\pi^-$ mass bins. The dashed histograms show the corresponding distributions for the $D_{s1}(2536)^+$ phase space decay in Monte Carlo.

ANGULAR ANALYSIS OF $D_{s1}(2536)^+ \rightarrow D^{*+}K_S^0$ DECAY.

The $D_{s1}(2536)^+ \rightarrow D^{*+}K_S^0$ decay can be described by three angles α , β and γ defined as shown in Fig. 4. The angles α and β are measured in the D_{s1}^+ rest frame with respect to the direction of the boost needed to go from the e^+e^- center of mass frame to the D_{s1}^+ rest frame. α is the angle between the boost direction and the K_S^0 momentum. β is the angle between the decay plane and the plane formed by the K_S^0 and the boost direction. The third angle γ is defined in the D^{*+} rest frame between π^+ and K_S^0 .

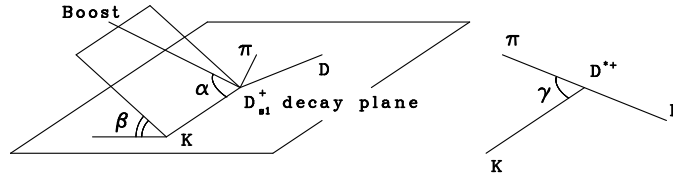


FIG. 4: Definitions of the angles α , β and γ . The first two are measured in the $D_{s1}(2536)^+$ rest frame, the last one – in the D^{*+} frame. “Boost” changes the e^+e^- center of mass system to the $D_{s1}(2536)^+$ frame.

The measured $\cos \alpha$, β and $\cos \gamma$ angular distributions are shown in Fig. 5. They represent the signal yield obtained from fits to the $D^{*+}K_S^0$ mass spectra in bins of individual angular variable. All Gaussian parameters except the normalization are fixed in the fit to the values obtained from the overall spectrum in Fig. 1. The first distribution is efficiency corrected

since there is a slight linear efficiency dependence on $\cos \alpha$: the relative difference between the values at -1 and $+1$ is about 12%. Since the differential distribution in $\cos \alpha$ includes only even powers of $\cos \alpha$, such a linear dependence does not induce any biases when integrating over the whole allowed interval $[-1, +1]$ and thus no dependence of the integrated efficiency on the initial polarization of $D_{s1}(2536)^+$. No significant efficiency dependence on β and $\cos \gamma$ is observed and therefore the corresponding two spectra in Fig. 5 are not efficiency corrected. One can see that the first two distributions are not flat. This means that $D_{s1}(2536)^+$ is produced polarized and that it does not decay in a pure S wave. The last distribution is more important. For a pure S or D wave decay it should either be flat or have the form $(1 + 3 \cos^2 \gamma)$, respectively. In the general case of interference between S and D wave amplitudes it becomes a linear combination of $\sin^2 \gamma$ and $\cos^2 \gamma$:

$$\frac{1}{N} \frac{dN}{d \cos \gamma} = \frac{1}{2} \left\{ R + (1 - R) \left(\frac{1 + 3 \cos^2 \gamma}{2} \right) + \sqrt{2R(1 - R)} \cos \phi (1 - 3 \cos^2 \gamma) \right\},$$

where $R = \Gamma_S / (\Gamma_S + \Gamma_D)$, $\Gamma_{S,D}$ are the S, D wave partial widths respectively, ϕ is the relative phase between the two amplitudes. This is similar to the case of $D_1^*(2420)^0 \rightarrow D^{*+} \pi^-$ and $D_1^*(2420)^+ \rightarrow D^{*0} \pi^+$ decays studied by CLEO [5].

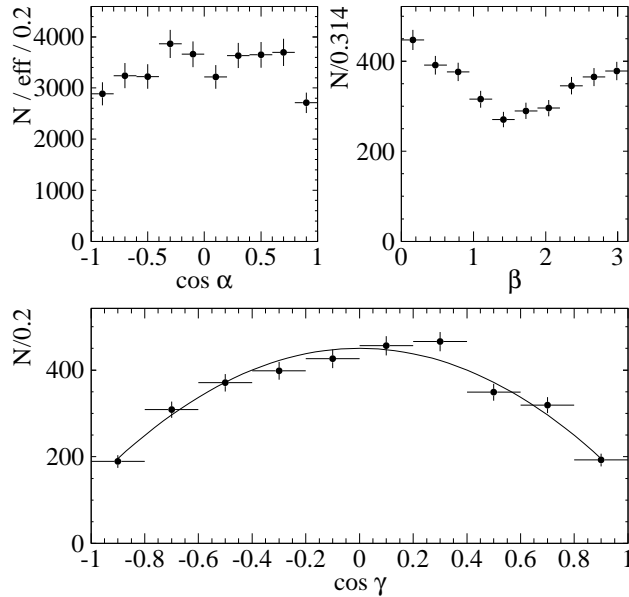


FIG. 5: Angular distributions for the $D_{s1}(2536)^+ \rightarrow D^{*+} K_S^0$ channel. The definitions of angles α , β and γ are given in the text and in Fig. 4. $D_{s1}(2536)^+$ reconstruction efficiency depends slightly on $\cos \alpha$, therefore the upper left plot is efficiency corrected. A fit to the $\cos \gamma$ distribution is described in the text.

Fitting the $\cos \gamma$ distribution in Fig. 5 to the form $1 + A \cos^2 \gamma$ yields $A = -0.70 \pm 0.03$ and a χ^2 per degree of freedom of 1.39. It was checked that the A parameter obtained on the subsamples defined by the cuts $\cos \alpha < 0$, $\cos \alpha > 0$, $\beta < \pi/2$, $\beta > \pi/2$, $x_P < 0.93$ or $x_P > 0.93$ agree with each other within statistical accuracy. Knowledge of A constrains the

contribution of S wave to the width and the relative phase ϕ :

$$\cos \phi = \frac{\frac{3-A}{3+A} - R}{2\sqrt{2R(1-R)}}.$$

The allowed range $|\cos \phi| \leq 1$ is shown in Fig. 6. Two lines in this plot bound the region which corresponds to $\pm 1\sigma$ deviation in A . Regardless of the value of ϕ , the S wave contribution is limited from below and from above by the values corresponding to $\phi = 0$. Conservatively taking the value of A to be 2σ below the central value, the limits obtained are:

$$0.277 < R < 0.955.$$

The corresponding limit for ϕ is: $|\phi| < 42^\circ$.

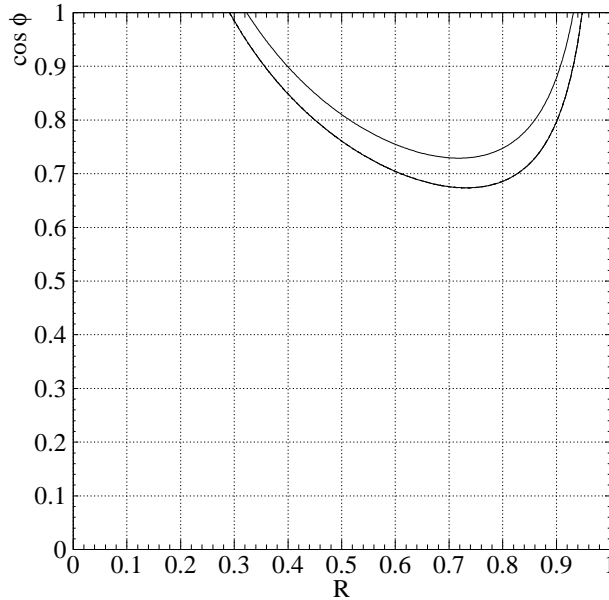


FIG. 6: Plot of cosine of the relative phase of S and D wave amplitudes in the $D_{s1}(2536)^+ \rightarrow D^{*+}K_S^0$ decay versus $R = \Gamma_S/(\Gamma_S + \Gamma_D)$. The two curves bound the region that corresponds to a $\pm 1\sigma$ deviation in the measured parameter A .

In conclusion, a new decay channel $D_{s1}(2536)^+ \rightarrow D^+\pi^-K^+$ is observed. The $D^+\pi^-$ pair is the only $D\pi$ combination that cannot come from a real D^* resonance. It can be produced in $D_{s1}(2536)^+$ two-body decays only through the virtual resonances D^{*0} , broad D_0^{*0} or $D_2^{*0}(2460)$. In addition, the $D^+\pi^-K^+$ final state can be formed by two-body decays to a D^+ and a virtual K^{*0} or higher K^* resonance. No clear resonant substructure is found in the $D^+\pi^-K^+$ system. The ratio of branching fractions $\frac{\mathcal{B}(D_{s1}(2536)^+ \rightarrow D^+\pi^-K^+)}{\mathcal{B}(D_{s1}(2536)^+ \rightarrow D^{*+}K_S^0)}$ is measured to be $(2.8 \pm 0.2 \pm 0.4)\%$. An angular analysis of the normalization decay $D_{s1}(2536)^+ \rightarrow D^{*+}K_S^0$ is also performed. The $D_{s1}(2536)^+$ may mix with another $J^P = 1^+, j = 1/2$ state, which is presumably the recently discovered $D_{sJ}(2460)^+$ meson and can decay in an S wave. Since the energy release in this reaction is small, the D wave is suppressed and the S wave can give a sizeable contribution to the total width even if the mixing is small. The measured

$1 - (0.70 \pm 0.03) \cos^2 \gamma$ D^{*+} helicity angular distribution constrains the relative fraction of the S wave component to the range $0.277 < R < 0.955$, independent of the phase ϕ .

We thank the KEKB group for the excellent operation of the accelerator, the KEK cryogenics group for the efficient operation of the solenoid, and the KEK computer group and the National Institute of Informatics for valuable computing and Super-SINET network support. We acknowledge support from the Ministry of Education, Culture, Sports, Science, and Technology of Japan and the Japan Society for the Promotion of Science; the Australian Research Council and the Australian Department of Education, Science and Training; the National Science Foundation of China under contract No. 10175071; the Department of Science and Technology of India; the BK21 program of the Ministry of Education of Korea and the CHEP SRC program of the Korea Science and Engineering Foundation; the Polish State Committee for Scientific Research under contract No. 2P03B 01324; the Ministry of Science and Technology of the Russian Federation; the Ministry of Higher Education, Science and Technology of the Republic of Slovenia; the Swiss National Science Foundation; the National Science Council and the Ministry of Education of Taiwan; and the U.S. Department of Energy.

-
- [1] B. Aubert *et al.* BaBar Collab., Phys. Rev. Lett. **90**, 242001 (2003);
D. Besson *et al.* CLEO Collab., Phys. Rev. **D68**, 032002 (2003);
P. Krokovny, *et al.* BELLE Collab., Phys. Rev. Lett. **91**, 262002 (2003);
A. Drutskoy *et al.* BELLE Collab., Phys. Rev. Lett. **94**, 061802 (2005).
 - [2] Y. Mikami *et al.* BELLE Collab., Phys. Rev. Lett. **92**, 012002 (2004).
 - [3] See P. Colangelo, F. De Fazio and R. Ferrandes, Mod. Phys. Lett. **A19**, 2083 (2004), and references therein.
 - [4] N. Isgur and M. Wise, Phys. Rev. Lett. **66**, 1130 (1991);
M. Lu, M. Wise and N. Isgur, Phys. Rev. **D45**, 1553 (1992).
 - [5] P. Avery *et al.* CLEO Collab., Phys. Lett. **B331**, 236 (1994), hep-ph/9403359, Erratum **B342** 453 (1995);
T. Bergfeld *et al.*, Phys. Lett. **B340**, 194 (1994).
 - [6] S. Kurokawa and E. Kikutani, Nucl. Instr. Meth. A **499**, 1 (2003).
 - [7] A. Abashian *et al.* (Belle Collab.), Nucl. Instr. and Meth. A **479**, 117 (2002).
 - [8] Y. Ushiroda (Belle SVD2 Group), Nucl. Instr. and Meth. A **511** 6 (2003).
 - [9] EvtGen home page <http://www.slac.stanford.edu/~lange/EvtGen>,
see also D. Lange, Nucl. Instr. and Meth. A **462** 152 (2001);
PYTHIA, T. Sjöstrand *et al.*, Computer Physics Commun. **135** 238 (2001), hep-ph/0308153;
GEANT, R. Brun *et al.*, GEANT 3.21, CERN Report DD/EE/84-1 (1984).
 - [10] S. Eidelman *et al.* (Particle Data Group), Phys. Lett. **B592**, 1 (2004).